Research Square

Preprints are preliminary reports that have not undergone peer review.
They should not be considered conclusive, used to inform clinical practice,
or referenced by the media as validated information.

Cell-state-resolved HLA class II regulation of serum IgA and its causal link to IgA nephropathy

Haoqi Shi
Nanjing Medical University
Jianhua Wu
wujoshua@ntu.edu.cn

Affiliated Hospital of Nantong University

Research Article

Keywords: Antigen presentation, Colocalization, Expression quantitative trait loci, HLA class II, IgA nephropathy, Mendelian randomization

Posted Date: November 26th, 2026

DOI: https://doi.org/10.21203/rs.3.rs-11731147/v1

License: This work is licensed under a Creative Commons Attribution 4.0 International License. Read Full License

Additional Declarations: No competing interests reported.

Abstract

Immunoglobulin A (IgA) nephropathy (IgAN) arises from excessive production of IgA, yet the immune cell states through which inherited variation acts on IgA levels remain unresolved. We integrated single-cell expression quantitative trait loci (eQTLs) from 24 immune cell subsets (OneK1K, n = 982 donors) with genome-wide association summary statistics for serum IgA levels (n = 41,263) and IgAN (10,146 cases, 28,751 controls). Using multi-variant inverse-variance-weighted Mendelian randomization (MR) and Bayesian colocalization, we first confirmed that genetically predicted serum IgA increases IgAN risk (odds ratio 2.26 per standard deviation, 95% confidence interval 1.87–2.75, $P = 1.5 \times 10^{-16}$; 17 instruments; weighted median 1.83; MR-Egger intercept P = 0.52). We then tested 7,442 gene–subset combinations for colocalization with serum IgA. Twenty-one colocalizations were identified across 11 of 24 subsets, and all mapped to the HLA region. Human leukocyte antigen (HLA) class II genes (HLA-DQB1, HLA-DRB1, HLA-DRB6, HLA-DRB9, HLA-DQA1, HLA-DQA2 and HLA-DMA) colocalized exclusively in professional antigen-presenting cells—naive and intermediate B cells, conventional dendritic cells and naive T cells—whereas class I and non-classical genes (HLA-A, HLA-C and HLA-E) colocalized in memory B cells, plasmablasts and regulatory T cells. Thirteen subsets, including both monocyte populations, plasmacytoid dendritic cells and hematopoietic progenitors, showed no colocalization. The same axis was recovered when IgAN was used as the outcome. These data indicate that inherited control of serum IgA is concentrated in HLA class II regulation within antigen-presenting cells, and provide a cell-state-resolved framework for the IgA–IgAN axis.

INTRODUCTION

Immunoglobulin A (IgA) nephropathy (IgAN) is the most common primary glomerulonephritis worldwide and a leading cause of kidney failure in young adults [1]. Its pathogenesis is best described by a multi-hit model: overproduction of galactose-deficient IgA1 by mucosal and systemic B cells (hit 1), generation of IgG autoantibodies against the aberrant hinge glycans (hit 2), and mesangial deposition of immune complexes with complement activation (hit 3) [2]. Genome-wide association studies (GWAS) have established that inherited susceptibility is dominated by the HLA region together with a limited set of non-HLA loci involved in mucosal immunity and complement regulation [3, 4].

Serum IgA level is the quantitative endophenotype closest to hit 1. A recent GWAS in 41,263 individuals identified 20 loci for serum IgA and reported that Mendelian randomization (MR) supports elevated serum IgA as a causal factor for IgAN [5]. That analysis used bulk blood eQTL resources for colocalization, which cannot assign regulatory effects to individual immune cell states, and summary-data-based MR with bulk eQTLs has likewise been applied to IgAN without cell-state resolution [15]. Because IgA production is confined to B cells and is regulated by T follicular helper and dendritic cell signals, cell-state resolution is essential for translating an HLA signal into a cellular mechanism.

Single-cell eQTL resources now make such resolution feasible. The OneK1K study profiled 982 donors across 24 immune cell types and identified thousands of cell-type-specific cis-eQTLs [6], and uniformly processed summary statistics are available through the eQTL Catalogue [7]. Here we combine these resources with serum IgA and IgAN GWAS to ask two questions: through which immune cell states does inherited variation act on serum IgA, and is the resulting axis visible at the disease end and in kidney tissue?

We deliberately treat the previously reported IgA-to-IgAN causal estimate as a replication target rather than a discovery claim [5], and focus our analysis on the cell-state architecture of the exposure end.

METHODS

Data sources

Single-cell eQTLs. Full cis-eQTL summary statistics for 24 immune cell types (OneK1K cohort, European donors) were obtained from the eQTL Catalogue (study QTS000038, 24 datasets; GRCh38) [6, 7]. Permutation-based eGene calls ($p_{perm} < 0.05$) were taken from the corresponding permuted tables and used to restrict testing to genes with a demonstrable cis effect in that subset.

Outcome and exposure GWAS. Serum IgA level GWAS summary statistics (41,263 individuals of diverse ancestries, 17 cohorts, fixed-effects meta-analysis) were obtained from the published resource [5]. IgAN GWAS summary statistics (10,146 cases, 28,751 controls) were obtained from the Kiryluk laboratory resource [4]. Both files are reported on GRCh37; eQTL variants (GRCh38) were mapped to GRCh37 with a UCSC chain file, requiring exact allele matches.

Tissue-level transcriptomics. GeoMx whole-transcriptome data from IgAN kidney biopsies (GSE311745; 29 regions of interest) were used for descriptive localization of the antigen-presentation module.

Instrument selection and Mendelian randomization of gene expression

For each gene–subset pair, cis variants were matched to the outcome GWAS by position and alleles. Variants with an F statistic below 10 were discarded, and the remainder were thinned to at least 20 kb spacing, retaining at most 30 variants; genes with fewer than two retained variants were analyzed for colocalization only. Multi-variant inverse-variance-weighted (IVW) estimates were computed with the first-order standard error [8], and Cochran's Q was used to quantify heterogeneity. We preferred IVW over summary-data-based MR [16] because the latter requires an ancestry-matched linkage-disequilibrium reference panel, which was not available locally.

Colocalization

Colocalization used the five-hypothesis framework with a single causal variant per region and the standard priors ($p1 = p2 = 1 \times 10^{-4}$, $p12 = 1 \times 10^{-5}$) [9]. For each gene, all matched regional variants were analyzed (position-thinned to a maximum of 6,000). Priors were widened for the case–control outcome by using the standard deviation of the latent liability ($sdY = 1/\sqrt{(s(1 - s))}$, with $s = 0.26$). Colocalization was declared at a posterior probability of H4 above 0.8. Our implementation was shown to reproduce R $coloc$ version 5.2.3 exactly on two simulated datasets and on real data (PP.H4 = 0.1321 by both implementations).

Two-sample MR for serum IgA on IgAN

Independent IgA-level variants ($P < 5 \times 10^{-8}$, thinned to 1 Mb) were used as instruments for IgAN. IVW was the primary estimator, with weighted median [10], MR-Egger regression [11] and leave-one-out analysis as sensitivity analyses [12].

Tissue module score

GeoMx counts were converted to log2 counts per million and averaged across regions of interest within each participant before group comparison; no inferential testing was performed because regions are nested within participants (E1, n = 4; E0, n = 3; normal, n = 3).

Software

Analyses were performed in Python 3.13 (NumPy, pandas, SciPy) and R 4.5.1 ($coloc$ 5.2.3). Scripts are available at available from the corresponding author upon reasonable request.

RESULTS

Analysis overview

We integrated 24 single-cell eQTL datasets with serum IgA and IgAN GWAS (Fig. 1). After restricting to permutation-defined eGenes and requiring at least ten matched regional variants, 7,442 gene–subset combinations were testable for colocalization with serum IgA. The serum IgA GWAS contributed 4,687 variants at genome-wide significance, which reduced to 20 independent instruments after 1 Mb thinning.

Genetically predicted serum IgA increases IgAN risk

Seventeen of the 20 IgA instruments were available in the IgAN GWAS with concordant alleles. IVW estimated an odds ratio of 2.26 per standard deviation of genetically predicted serum IgA (95% CI 1.87–2.75; $P = 1.5 \times 10^{-16}$; Fig. 1A, Table 2). The weighted median estimate was concordant (OR 1.83), the MR-Egger intercept showed no evidence of directional pleiotropy (+ 0.011, P = 0.52), and leave-one-out estimates ranged from 0.71 to 0.97 on the log scale. Excluding the strongest instrument, a variant near 1p36 with a large effect on IgA but no detectable effect on IgAN, increased the estimate to 2.65 (95% CI 2.14–3.27). This reproduces the direction and magnitude previously reported for the same exposure [5].

Table 2
Mendelian randomization of genetically predicted serum IgA on IgAN.

Analysis	Estimate	95% CI	P
IVW (17 instruments)	OR 2.26	1.87–2.75	1.5×10^{-16}
Weighted median	OR 1.83	—	—
MR-Egger intercept	+ 0.011	—	0.52
Leave-one-out range (β)	0.71–0.97	—	—
Excluding 1p36 instrument	OR 2.65	2.14–3.27	2.2×10^{-19}
Supplementary Table S4. Cell-state eQTL effects of the Gd-IgA1 lead variant rs13226913 on C1GALT1.			

[Table 2 near here]

Colocalization with serum IgA is restricted to the HLA region

Of the 7,442 tests, 21 gene–subset pairs reached PP.H4 > 0.8, distributed across 11 of the 24 subsets. Every colocalized gene mapped to the HLA region on chromosome 6 (Table 1, Fig. 1B).

Table 1
Gene–cell-state pairs colocalizing with serum IgA level (PP.H4 > 0.8).

Cell state	Gene	Ensembl	Matched cis variants	Instruments	IVW β	IVW P	PP.H4
B intermediate	HLA-DRB1	ENSG00000196126	13	5	−0.009	0.74	0.964
B intermediate	HLA-DRB6	ENSG00000229391	13	5	0.009	0.69	0.931
B intermediate	HLA-DQA2	ENSG00000237541	12	4	0.005	0.84	0.930
B memory	HLA-C	ENSG00000204525	38	6	0.116	< 0.001	0.996
B naive	HLA-DRB6	ENSG00000229391	31	6	0.033	< 0.001	0.997
B naive	HLA-DQB1	ENSG00000179344	31	6	−0.007	0.75	0.996
B naive	HLA-DRB9	ENSG00000196301	33	6	0.045	0.002	0.992
B naive	DAXX	ENSG00000204209	84	2	0.321	< 0.001	0.895
B naive	ENSG00000248993	ENSG00000248993	29	1	—	—	0.868
CD4 TCM	ENSG00000285799	ENSG00000285799	47	9	0.016	0.25	0.981
CD4 naive	HLA-DQB1	ENSG00000179344	90	6	0.083	< 0.001	0.999
CD4 naive	HLA-DMA	ENSG00000204257	23	3	0.246	< 0.001	0.976
CD8 TEM	HLA-DRB6	ENSG00000229391	24	7	0.034	< 0.001	0.999
CD8 TEM	ENSG00000285761	ENSG00000285761	45	2	−0.188	< 0.001	0.873
CD8 naive	HLA-DQB1	ENSG00000179344	113	4	0.145	< 0.001	0.999
NK	ENSG00000285799	ENSG00000285799	47	6	0.086	< 0.001	0.982
NK	ENSG00000285761	ENSG00000285761	45	3	−0.153	< 0.001	0.971
Treg	HLA-E	ENSG00000204592	116	1	—	—	0.893
cDC2	HLA-DQA1	ENSG00000196735	43	6	0.071	< 0.001	0.999
cDC2	HLA-DQB1	ENSG00000179344	43	6	−0.002	0.94	0.899
plasmablast	HLA-A	ENSG00000206503	46	6	−0.070	< 0.001	0.965

The distribution of PP.H4 was strongly bimodal: no non-HLA gene exceeded 0.8, and the highest non-HLA value was 0.64.

[Table 1 near here]

Class II and class I genes partition by cell state

The colocalizing genes separated cleanly by antigen-presentation pathway and cell state. Class II genes—HLA-DQB1, HLA-DRB1, HLA-DRB6, HLA-DRB9, HLA-DQA1, HLA-DQA2 and HLA-DMA—colocalized only in professional antigen-presenting cells: naive B cells (five genes; PP.H4 0.87–1.00), intermediate B cells (three genes; 0.93–0.96), conventional dendritic cells (HLA-DQA1, PP.H4 0.999; HLA-DQB1, 0.90), naive CD4 T cells (HLA-DMA, 0.98; HLA-DQB1, 1.00) and naive CD8 T cells (HLA-DQB1, 0.999). In contrast, class I and non-classical genes were confined to effector and memory compartments: HLA-C in memory B cells (PP.H4 0.996), HLA-A in plasmablasts (0.965) and HLA-E in regulatory T cells (0.893) (Fig. 1B, 1C).

HLA-DQB1 and HLA-DRB6 each colocalized in four independent subsets, indicating a shared class II regulatory architecture rather than a subset-private effect.

Thirteen subsets showed no colocalization at all, including CD14 and CD16 monocytes, plasmacytoid dendritic cells, MAIT cells, γδ T cells, hematopoietic progenitors, both natural killer subsets and platelets (Fig. 1C).

Both dimensions of evidence are required

IVW significance and colocalization were largely independent (Fig. 1E). Several genes reached strong IVW P values without colocalizing, and conversely HLA-DQB1 in intermediate B cells colocalized despite a null IVW estimate (P = 0.74), reflecting a single shared signal in which the ratio estimate is imprecise. Restricting inference to genes satisfying both criteria yielded the same 21 pairs, all HLA.

The same axis is recovered at the disease end

When IgAN replaced serum IgA as the outcome, 25 gene-subset pairs colocalized across 12 subsets and again concentrated in the HLA region and in B-cell states: HLA-DQA2 (PP.H4 0.998), HLA-DQB2 (0.998) and TSBP1-AS1 (0.999) in naive B cells, HLA-DQB1 (0.997) and HLA-DRA (0.992) in intermediate B cells, and HLA-B (0.998) in memory B cells (Fig. 2). AIF1, a gene prioritized for IgAN in a proteome-wide study [13], colocalized in CD4 T cells (PP.H4 0.994), providing an independent directional check on the approach.

The galactose-deficiency locus acts as a cell-state-dependent C1GALT1 eQTL

Full genome-wide summary statistics for galactose-deficient IgA1 (Gd-IgA1) are not publicly available: the only Gd-IgA1 GWAS (2,633 individuals) reports two genome-wide significant loci and curated top hits but no complete summary statistics, so the Gd-IgA1 MR and colocalization pipeline could not be applied. We therefore interrogated the established locus directly. The lead variant at C1GALT1, rs13226913, was a cis-eQTL for C1GALT1 in 7 of 17 testable subsets (Table S4). Effects ranged from $\beta = 0.007$ per copy in naive CD8 T cells to $\beta = 0.201$ in central memory CD4 T cells, with the strongest signals in central memory CD4 T cells ($P = 1.6 \times 10^{-9}$) and NK cells ($P = 5.7 \times 10^{-9}$); naive B cells also showed a clear effect ($\beta = 0.174$, $P = 9.4 \times 10^{-6}$). Effects were heterogeneous across subsets (Cochran $Q = 55.0$, $df = 16$, $P = 3.5 \times 10^{-6}$) but did not differ between B-lineage and non-B subsets ($P = 0.87$). The sign is consistent with the reported biology, in which the Gd-IgA1-increasing allele lowers C1GALT1 expression. Because detectability depends jointly on eQTL strength and subset sample size, we regard the gradient as suggestive rather than established.

Kidney tissue shows a coordinated antigen-presentation module

In glomerular regions of interest, transcripts of the antigen-presentation module were coordinately lower in E1 compared with E0 lesions: HLA-DMA − 0.71, CD74 − 0.60, HLA-DRB1 − 0.58 and HLA-DQB1 − 0.49 log2 CPM (Fig. 1D). The direction was consistent across five genes, indicating a module-level rather than gene-specific difference; because regions are nested within a small number of participants, this observation is descriptive.

DISCUSSION

We show that inherited control of serum IgA, the quantitative trait closest to the first hit of IgAN pathogenesis, is concentrated in HLA class II regulation within professional antigen-presenting cells and is absent from thirteen of twenty-four immune subsets. The IgA-to-IgAN causal estimate that anchors the chain reproduces the published result [5]; the new information lies in where, within the immune system, that regulation acts.

Two observations are worth emphasizing. First, the class II/class I partition follows the biology of antigen presentation rather than lineage labels: class II genes colocalized in naive and intermediate B cells, conventional dendritic cells and naive T cells, whereas class I genes appeared in memory B cells, plasmablasts and regulatory T cells. This is consistent with a model in which the inherited component of IgA production operates at the initiation of T-dependent B-cell responses rather than at the terminal plasma-cell stage. Second, the complete absence of signal in monocytes, plasmacytoid dendritic cells and progenitors argues against a generic myeloid or inflammatory explanation and supports the specificity of the finding.

The virtual absence of non-HLA colocalization deserves comment. Serum IgA loci outside the HLA region, including TNFSF13B and TNFRSF13B, were not recoverable at this resolution, in part because these genes are not permutation-defined eGenes in most circulating subsets and in part because the IgA GWAS offers fewer variants for matching than the IgAN GWAS. We therefore interpret our map as a lower bound on cell-state resolution rather than as a complete catalogue.

Our findings should be read with several limitations in mind. Variants were thinned by distance rather than by linkage disequilibrium because no ancestry-matched LD panel was available locally; consequently IVW P values are anti-conservative and inference was anchored on colocalization, which does not require LD. Colocalization assumed a single causal variant per region and analyzed up to 6,000 variants per gene; although the implementation reproduces R $coloc$ exactly on identical input, regional truncation may slightly inflate H4. The HLA region carries extreme linkage disequilibrium, so class II colocalization cannot distinguish among neighbouring genes; the reported genes should be regarded as a haplotype-level signal. Only 20 independent IgA instruments were available after 1 Mb thinning, which limits precision, although all sensitivity analyses were concordant. Finally, the tissue-level observation is descriptive and cannot establish directionality, and the glycosylation analysis is restricted to two established loci because genome-wide Gd-IgA1 summary statistics are unavailable, which prevents any statement about the genome-wide architecture of galactose deficiency.

At the glycosylation step, the established C1GALT1 variant behaves as a cell-state-dependent eQTL that is strongest in central memory CD4 T cells and NK cells rather than in B cells, which raises the possibility that the inherited component of IgA galactose deficiency is partly regulated outside the antibody-secreting compartment. Formal testing of that hypothesis requires Gd-IgA1 summary statistics at genome-wide scale, which are not currently public.

These results suggest a reframing of the IgA–IgAN axis for genetic study: rather than searching for non-HLA causal genes in blood immune cells, effort may be better directed at the antigen-presentation programme of mucosal and kidney-draining B-cell and dendritic-cell populations, using compartment-resolved kidney eQTL resources such as NephQTL [14] to close the gap between circulating and tissue-resident regulation. Clinically, the concentration of signal

in class II antigen presentation is compatible with the observed heterogeneity of responses to B-cell–directed therapies and motivates cell-state-resolved pharmacogenetic analyses.

Declarations

Ethics statement. This study used only publicly available, de-identified summary statistics and therefore did not require institutional review board approval.

Conflict of interest.

The authors declare no competing interests.

Funding.

This work was supported by the Foundation of Jiangsu Province Research Hospital (grant number YJXYY202204-XKB13). The funders had no role in study design, data collection, analysis, interpretation, or the decision to submit the manuscript for publication.

Author Contribution

Jianhua Wu: funding acquisition, project administration, resources, supervision, writing - review and editing. Haoqi Shi: conceptualization, data curation, formal analysis, investigation, methodology, software, validation, visualization, writing - original draft, writing - review and editing. Both authors read and approved the final manuscript.

Acknowledgement

We thank the OneK1K study, the eQTL Catalogue, the Kiryluk laboratory for public summary statistics, and the NEPTUNE and CureGN consortia for kidney tissue data.

Data availability.

All data are publicly available. Single-cell eQTL summary statistics: eQTL Catalogue study QTS000038 (https://www.ebi.ac.uk/eqtl/). Serum IgA GWAS: https://www.columbiamedicine.org/divisions/kiryluk/study_gwas_stat_IgA.php (file META.IGA.LEVELS.ALL.COMBINED.txt). IgAN GWAS: https://www.columbiamedicine.org/divisions/kiryluk/. GeoMx data: GEO GSE311745. Analysis code: available from the corresponding author upon reasonable request.

References

1. Wyatt RJ, Julian BA. IgA nephropathy. N Engl J Med 2013;368:2402–2414.
2. Suzuki H, Kiryluk K, Novak J, Moldoveanu Z, Herr AB, Renfrow MB, et al. The pathophysiology of IgA nephropathy. J Am Soc Nephrol 2011;22:1795–1803.
3. Kiryluk K, Li Y, Scolari F, Sanna-Cherchi S, Choi M, Verbitsky M, et al. Discovery of new risk loci for IgA nephropathy implicates genes involved in immunity against intestinal pathogens. Nat Genet 2014;46:1187–1196.

4. Kiryluk K, Sanchez-Rodriguez E, Zhou XJ, Zanoni F, Liu L, Mladkova N, et al. Genome-wide association analyses define pathogenic signaling pathways and prioritize drug targets for IgA nephropathy. Nat Genet 2023;55:1091–1105.
5. Liu L, Khan A, Sanchez-Rodriguez E, Zanoni F, Li Y, Steers N, et al. Genetic regulation of serum IgA levels and susceptibility to common immune, infectious, kidney, and cardio-metabolic traits. Nat Commun 2023;14:655.
6. Perez RK, Gordon MG, Subramaniam M, Kim MC, Hartoularos GC, Targ S, et al. Single-cell RNA-seq reveals cell type-specific molecular and genetic associations to lupus. Science 2022;376:eabf1970.
7. Kerimov N, Hayhurst JD, Peikova K, Manning JR, Walter P, Kolberg L, et al. A compendium of uniformly processed human gene expression and splicing quantitative trait loci. Nat Genet 2021;53:1290–1299.
8. Burgess S, Butterworth A, Thompson SG. Mendelian randomization analysis with multiple genetic variants using summarized data. Genet Epidemiol 2013;37:658–665.
9. Giambartolomei C, Vukcevic D, Schadt EE, Franke L, Hingorani AD, Wallace C, et al. Bayesian test for colocalisation between pairs of genetic association studies using summary statistics. PLoS Genet 2014;10:e1004383.
10. Bowden J, Davey Smith G, Haycock PC, Burgess S. Consistent estimation in Mendelian randomization with some invalid instruments using a weighted median estimator. Genet Epidemiol 2016;40:304–314.
11. Burgess S, Thompson SG. Interpreting findings from Mendelian randomization using the MR-Egger method. Eur J Epidemiol 2017;32:377–389.
12. Hemani G, Zheng J, Elsworth B, Wade KH, Haberland V, Baird D, et al. The MR-Base platform supports systematic causal inference across the human phenome. eLife 2018;7:e34408.
13. Liu X, Hu Y, Zhang W, Nie C, Zhang F, Liu Y, et al. Integrating multiple omics approaches to identify AIF1 as a protective factor in IgA nephropathy. J Transl Autoimmun. 2026;13:100407.
14. Gillies CE, Putler R, Menon R, Otto E, Yasutake K, Nair V, et al. An eQTL landscape of kidney tissue in human nephrotic syndrome. Am J Hum Genet 2018;103:232–245.
15. Zhang Q, Zhang K, Zhu Y, Yuan G, Yang J, Zhang M. Exploring genes for immunoglobulin A nephropathy: a summary data-based mendelian randomization and FUMA analysis. BMC Med Genomics 2023;16:16.
16. Zhu Z, Zhang F, Hu H, Bakshi A, Robinson MR, Powell JE, et al. Integration of summary data from GWAS and eQTL studies predicts complex trait gene targets. Nat Genet 2016;48:481–487.

Figures

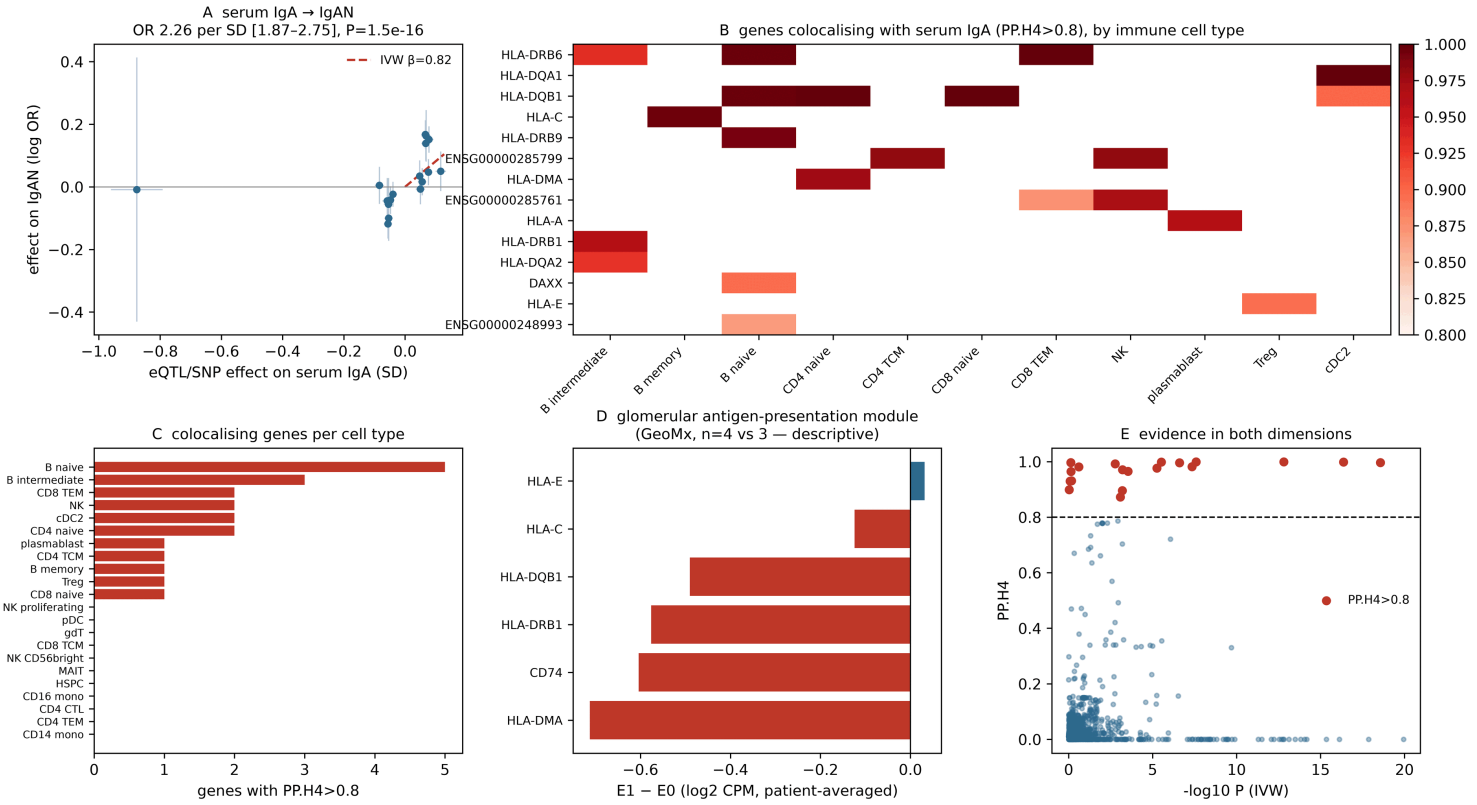


Figure 1

Cell-state-resolved regulation of serum IgA and its causal link to IgAN. (A) Scatter of instrument effects on serum IgA (x-axis) against effects on IgAN (y-axis); the dashed line shows the IVW slope (β = 0.82, OR 2.26 per SD). (B) Heatmap of posterior probabilities of a shared causal variant (PP.H4) between serum IgA and each cell state, shown for genes exceeding 0.8. (C) Number of colocalizing genes per cell state, ordered by count; thirteen subsets showed none. (D) Glomerular antigen-presentation module in E1 versus E0 lesions (GeoMx; patient-averaged log2 CPM; descriptive). (E) Relationship between IVW significance and PP.H4; red points indicate PP.H4 > 0.8.

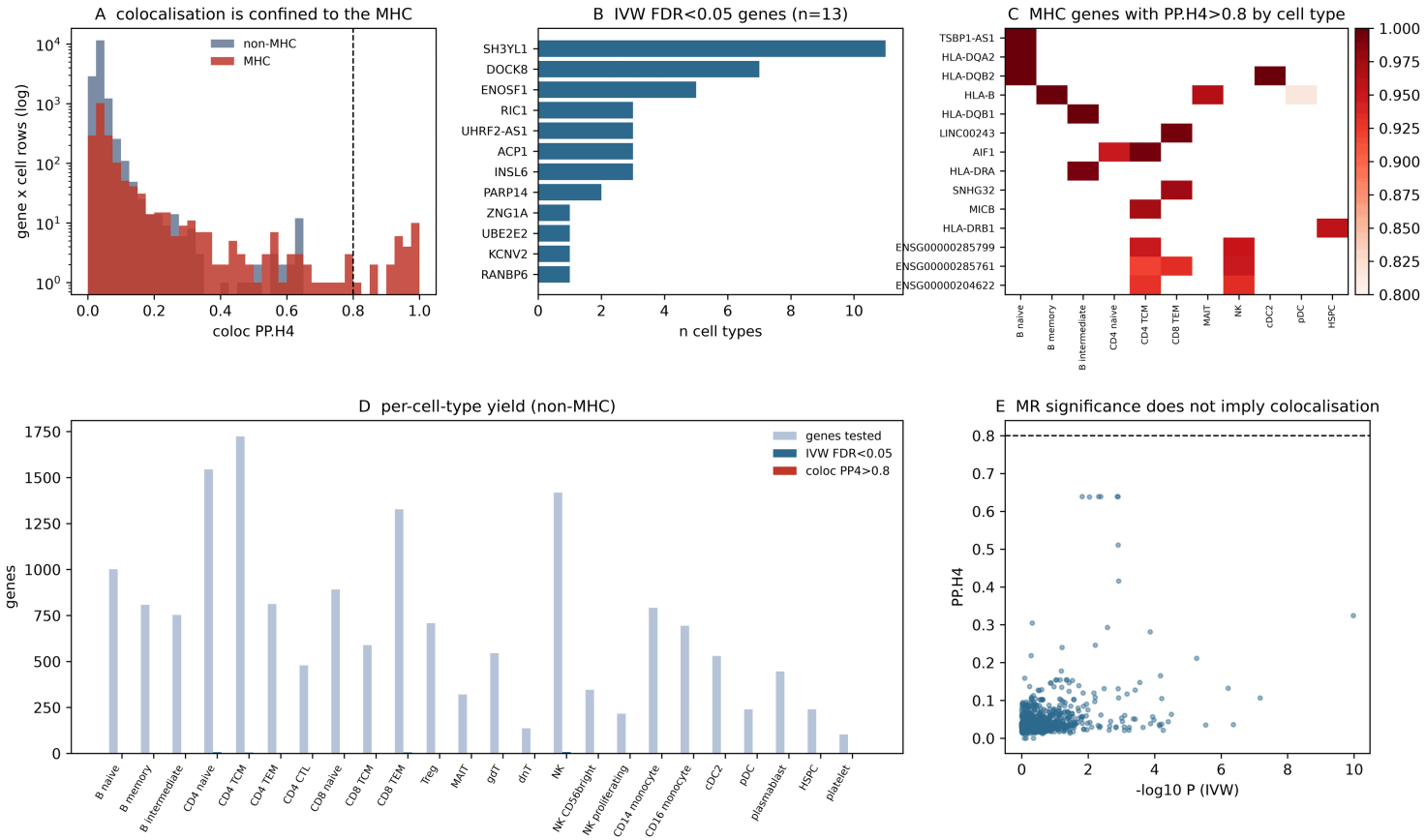


Figure 2

Colocalization with IgAN at the disease end. Per-cell-state counts of colocalizing genes with PP.H4 > 0.8 (non-MHC and MHC shown separately) and the IVW–colocalization relationship for the IgAN outcome.

Supplementary Files

This is a list of supplementary files associated with this preprint. Click to download.

- SupplementaryTables.xlsx